International Journal of Thermophysics, Vol. 5, No. 4, 1984

Thermal Conductivity of Hydrogen for Temperatures Between 78 and 310 K with Pressures to 70 MPa

H. M. Roder[1]

Received April 4, 1984

The paper presents new experimental measurements of the thermal conductivity of hydrogen. The ortho-para compositions covered are normal, near normal, para, and para-rich. The measurements were made with a transient hot wire apparatus. The temperatures covered the range from 78 to 310 K with pressures to 70 MPa and densities from 0 to a maximum of 40 mol · L^{-1}. For compositions normal and near normal, the isotherms cover the entire range of pressure, and the temperatures are 78, 100, 125, 150, 175, 200, 225, 250, 275, 294, 300, and 310 K. The para measurements include eight isotherms at temperatures from 100 to 275 K with intervals of 25 K, pressures to 12 MPa, and densities from 0 to 12 mol · L^{-1}. Three additional isotherms at 150, 250, and 275 K cover para-rich compositions with para percentages varying from 85 to 72%. For these three isotherms the pressures reach 70 MPa and the density a maximum of 30 mol · L^{-1}. The data for all compositions are represented by a single thermal conductivity surface. The data are compared with the experimental measurements of others through the new correlation. The precision (2σ) of the hydrogen measurements is between 0.5 and 0.8% for wire temperature transients of 4 to 5 K, while the accuracy is estimated to be 1.5%.

KEY WORDS: hot wire; hydrogen; normal hydrogen; ortho hydrogen; parahydrogen; thermal conductivity; transient; measurements.

1. INTRODUCTION

Values of the thermal conductivity of hydrogen at high pressures have been of considerable interest to the nation's space program for some time. In addition, the thermal conductivity of hydrogen, as it differs for ortho and para states, is a property of fundamental interest in developing the theory of

[1] Chemical Engineering Science Division, National Bureau of Standards, Boulder, Colorado 80303, U.S.A.

0195-928X/84/1200-0323$03.50/0

fluids. Accurate measurements of thermal conductivity are of considerable difficulty. Methods and geometries abound, each with its adherents and its inherent drawbacks. The steady state hot wire experiment is one of the older, well-established methods. The transient hot wire method used here has come into its own only with recent advances in digital electronics. The evolution of the modern transient hot wire experiment is traced in an earlier paper [1] where a complete description of the apparatus is given.

For the H_2 molecule, two spin isomers exist, orthohydrogen and parahydrogen. The differentiating feature is the relative orientation of the two nuclear spins of the molecule. The spins may be either parallel or antiparallel. Nuclear spin is a quantized motion with quantum numbers for the spin and quantized energy levels. Molecules with antiparallel nuclear spins, called parahydrogen, have even quantum numbers and are in the lowest energy state. Hydrogen may be thought of as a binary mixture of two different species of molecules differing from each other in nuclear spin and in physical properties. The equilibrium composition of the ortho-para concentration in the mixture is temperature dependent. For example, at a temperature of about 20 K, the equilibrium composition is 99.79% para and 0.21% ortho. Near ambient temperature the composition is 25% para and 75% ortho. This 25–75 composition is called normal hydrogen. A classic text on hydrogen is the book by Farkas [2].

A search of the literature reveals a reltive abundance of papers on the thermal conductivity of hydrogen [3]. However, measurements on normal hydrogen that cover a wide range in both temperature and density or pressure are rare [4, 5] and, as we shall see, differ considerably. Measurements on parahydrogen are extremely rare [4]; measurements on compositions other than 25% and 99.79% para are nonexistent. It is, therefore, not surprising that efforts to correlate the thermal conductivity surface of parahydrogen [6] are beset with difficulties, and that the results are occasionally in error by up to 25%.

In this paper new experimental measurements are presented for hydrogen compositions near normal that cover a large range in density for every isotherm, i.e., 0–19 mol · L^{-1} for 310 K and 0–40 mol · L^{-1} for 78 K. For the para composition the new measurements cover 8 isotherms with a density range of 0–8 mol · L^{-1} up to a range of 0–12 mol · L^{-1}. For pararich compositions these isotherms cover densities up to 30 mol · L^{-1}. The new results overlap our earlier measurements [4] and extend them to 300 K. The earlier measurements were done primarily at temperatures below 100 K. A part of the normal hydrogen measurements in preliminary form have been presented elsewhere [7], as well as averaged results of the para measurements [8].

The results are analyzed and used to develop a new correlation for the

thermal conductivity surface of hydrogen. The new correlation is valid for temperatures between 78 and 310 K, pressures between 0 and 70 MPa, and for all ortho-para compositions. For the dilute gas an existing critical evaluation and correlation by Hanley et al. [9] is used, but modified slightly. Differences due to ortho-para composition are accounted for in the dilute gas term. The excess thermal conductivity is described with a term similar to that used for oxygen [10]. A slight indication of a critical enhancement at the very lowest temperature is noted.

2. METHOD AND APPARATUS

The measurements were made with a transient hot wire thermal conductivity apparatus. This instrument has been tested with nitrogen and helium [1], and also with argon [11, 12]. It has been used to measure the thermal conductivity surfaces of oxygen [10] and propane [13]. A detailed description of the apparatus, of the experimental procedure, of the wire calibration, of the data reduction, and of the apparatus performance are given in the apparatus paper [1]. Several changes adopted for the measurements on oxygen [10] are retained here. These changes are a digital filter applied to the voltages measured across the bridge, and a linear deviation plot of the experimental temperature rises.

Several major changes had to be made to the apparatus after the original series of measurements on normal hydrogen. Between the original and the second series on hydrogen, a high pressure leak developed. After the repair, both long and short hot wires, thermocouples, and heaters had to be replaced. The temperature-resistance calibration of the new wires was defined by the second series of measurements on normal hydrogen, the new measurements on parahydrogen, and measurements on methane [14]. Before the measurements on methane could be completed, a problem with the high vacuum intervened. Heat lamps directed at the high pressure cell remedied the vacuum problem, but also caused a partial annealing of the hot wires, i.e., a shift in the temperature-resistance calibration. After the methane measurements were completed, a final series of measurements on normal hydrogen was made to determine the extent of the ortho-para conversion which occurs during the normal measurements at the lower temperatures. In effect the hydrogen measurements have to be divided into three series with a different wire calibration for each series as follows: first series, normal hydrogen, wire calibration as in ref. [1]; second series, normal and parahydrogen, new wires in the "as received" state; third series, normal hydrogen, new wires partially annealed. For the second and third series of measurements, a cubic equation in temperature is used to represent the wire

calibration. The pressure dependent term used earlier [1] is still statistically significant and is retained. The new wire equation is

$$R(T) = A + BT + CT^2 + DT^3 + EP \tag{1}$$

where T is the temperature in kelvins and P is the pressure in MPa. Calibration constants and wire resistances of the new wires both "as received" and partially annealed are given in Table I and II.

The samples used are research grade hydrogen stated by the supplier to be a minimum of 99.999 mol % hydrogen. Normal hydrogen samples taken directly from the supply bottle were routed through a molecular sieve and a 65 μm line filter to a small diaphragm compressor. Ortho-para conversion occurs while the normal sample is in the experimental cell. Final para concentrations increase above the initial 25% para depending on the experimental temperature. Nominally pure parahydrogen, i.e., a 20.4 K equilibrium of 99.79% para, was obtained by running the samples from the supply bottle through an ortho-para catalyst directly into the cell. The catalyst was cooled with liquid parahydrogen, at approximately 20 K. Completion of the conversion was verified with an ortho-para analyzer [15].

Table I. Calibration Constants of the Hot Wires

		As received	Partially annealed
Long wire	Temperature range, K	97–311	101–293
	Number of points in fit	1309	677
	Coefficients		
	A, Ω	−0.10650760E+02	−0.11266338E+02
	$B, \Omega \cdot K^{-1}$	0.37430571E+00	0.38014474E+00
	$C, \Omega \cdot K^{-2}$	−0.15288954E−03	−0.18332389E−03
	$D, \Omega \cdot K^{-3}$	0.13830261E−06	0.18822293E−06
	$E, \Omega \cdot MPa^{-1}$	−0.15128962E−02	−0.11316796E−02
	Standard deviation of fit, σ	0.17E−01	0.14E−01
	Equivalent error in T, K	0.045	0.036
Short wire	Temperature range, K	97–311	101–293
	Number of points in fit	1309	677
	Coefficients		
	A, Ω	−0.50441092E+01	−0.54906672E+01
	$B, \Omega \cdot K^{-1}$	0.17734574E+00	0.18254991E+00
	$C, \Omega \cdot K^{-2}$	−0.71544303E−04	−0.97358369E−04
	$D, \Omega \cdot K^{-3}$	0.64186692E−07	0.10494293E−06
	$E, \Omega \cdot MPa^{-1}$	−0.79965350E−03	−0.73849295E−03
	Standard deviation of fit, σ	0.17E−01	0.17E−01
	Equivalent error in T, K	0.094	0.091

Table II. Wire Resistances as a Function of Temperature

Pressure (MPa)	Temperature (K)	Wire resistences		Wire lengths		Resistances/unit length		Percent difference
		Long wire (Ω)	Short wire (Ω)	Long wire (cm)	Short wire (cm)	Long wire ($\Omega \cdot cm^{-1}$)	Short wire ($\Omega \cdot m^{-1}$)	
				As received				
0.1013	100.0	25.3891	12.0391	10.477	4.981	242.3	241.7	0.27
0.1013	125.0	34.0185	16.1315	10.479	4.982	324.6	323.8	0.27
0.1013	150.0	42.5217	20.1646	10.481	4.983	405.7	404.6	0.27
0.1013	175.0	50.9116	24.1443	10.483	4.984	485.7	484.4	0.26
0.1013	200.0	59.2011	28.0767	10.485	4.985	564.6	563.2	0.26
0.1013	225.0	67.4032	31.9678	10.487	4.986	642.7	641.1	0.25
0.1013	250.0	75.5309	35.8236	10.490	4.988	720.1	718.3	0.25
0.1013	273.0	83.0021	39.3679	10.492	4.989	791.1	789.2	0.25
0.1013	275.0	83.5971	39.6502	10.492	4.989	796.8	794.8	0.25
0.1013	300.0	91.6149	43.4536	10.494	4.990	873.0	870.8	0.25
0.1013	325.0	99.5972	47.2397	10.497	4.991	948.8	946.5	0.25
				Partially annealed				
0.1013	100.0	25.1030	11.8956	10.477	4.981	239.6	238.8	0.34
0.1013	125.0	33.7548	16.0117	10.479	4.982	322.1	321.4	0.24
0.1013	150.0	42.2657	20.0554	10.481	4.983	403.3	402.5	0.21
0.1013	175.0	50.6533	24.0363	10.483	4.984	483.2	482.2	0.20
0.1013	200.0	58.9353	27.9644	10.485	4.985	562.1	560.9	0.21
0.1013	225.0	67.1293	31.8496	10.487	4.986	640.1	638.7	0.22
0.1013	250.0	75.2530	35.7016	10.490	4.988	717.4	715.8	0.22
0.1013	273.0	82.7281	39.2475	10.492	4.989	788.5	786.7	0.22
0.1013	275.0	83.3239	39.5302	10.492	4.989	794.2	792.4	0.22
0.1013	300.0	91.3598	43.3454	10.494	4.990	870.6	868.7	0.22

For these measurements the maximum pressure is about 12 MPa (1800 psia). The measurements on para-rich mixtures were made by running the parahydrogen from the ortho-para catalyst through the diaphragm compressor. The compressor converted some of the para back to ortho, yielding an initial para concentration around 80%. Additional conversion occurs while the sample is in the experimental cell so that the final para concentrations were around 75%.

3. RESULTS

To define the thermal conductivity surface of hydrogen in the region of interest, a grand total of 1707 points were measured. Of these, 20 points were taken to determine the onset of convection experimentally. Another 42 points were rejected for experimental reasons such as insufficient experimental time of measurement, inadequate equilibrium, experimental density too low, $\Delta T - \ln(t)$ relation not linear enough, etc. The remaining 1645 valid points are distributed among 12 isotherms as shown in Table III. These valid points fall into three series. The initial series of 585 points on normal and near normal compositions was measured with the original set of

Table III. Summary Table of Hydrogen Thermal Conductivity Measurements

Nominal temp. K	Number of points			
% para:	Normal (25)[a]	Near normal (25–50)	Para (99.79)	Para-rich (85–72)
78		81 [1]		
100	36 [3][b]	68 [1]	32 [2]	
125	40 [3]	72 [1], 92 [3]	32 [2]	
150		63 [1]	36 [2]	96 [2]
175		73 [1]	35 [2]	
200		66 [1]	36 [2]	
225		95 [2]	38 [2]	
250	70 [1]		36 [2]	82 [2]
275	92 [2]		24 [2]	63 [2]
294	98 [2]			
300	92 [1]			
313.5	97 [2]			
Totals:	525	610	269	241

[a] Numbers in parentheses are % para.
[b] Series of the measurements in brackets.

wires. After the apparatus had been rebuilt, a second series, an additional 382 points on normal hydrogen and 510 points on para and para-rich compositions, were measured with the new wires. The third series, also with the new wires but after they had been partially annealed, was measured on normal and near-normal compositions to define the effect of changes in ortho-para composition.

Measurements on each isotherm were made at a number of different pressure levels. At each pressure level several different power levels were used, resulting in slightly different experimental temperatures and densities. For the first series on normal hydrogen, there are roughly 72 points per isotherm, taken at 24 different pressure levels, with three different power levels at each pressure. For the second and third series on normal hydrogen, there are also about 24 different pressure levels with, however, four different power levels at each pressure. The eight short para isotherms have eight or nine different pressure levels with four different power levels; the para-rich isotherms have 24 pressure levels and four power levels.

For any given experimental point, the pressure, cell temperature, and applied power are measured directly. The experimental temperature and the thermal conductivity with its associated regression error are obtained through the data reduction program, while the density is calculated from an equation of state [16] using the measured pressure and the experimental temperature. We note that the experimental temperatures vary with the applied power and are several degrees higher than the cell temperature. The ortho-para composition is assigned by analysis (see Section 4.2).

An overview of the adjusted thermal condutvctivities on even isotherms is given in Fig. 1, where the lines are the isotherms calculated from the correlation. Isotherms for normal hydrogen, for parahydrogen, and for para-rich mixtures are plotted vs density in separate panels in Fig. 1. The end points of each isotherm at zero density, the dilute gas values, are plotted in a third panel vs temperature to show the differences between normal and parahydrogen clearly.

A complete table which includes all 1645 experimental measurements is given in ref. [17]. In this paper, to conserve space, Table AI (as an Appendix) presents a summary of thermal conductivity values obtained by averaging the temperatures, densities, para compositions, and thermal conductivities for the three or four power levels at any given pressure level. In much of the subsequent analysis, it is desirable to have the thermal conductivities at integral values of temperature. Therefore, each point was adjusted at constant density to the nominal isotherm temperature by a slight shift in temperature using the correlating equation given in Section 4.5.

The replicate measurements at the same cell temperature and pressure with different power levels serve to verify the absence of convection. The

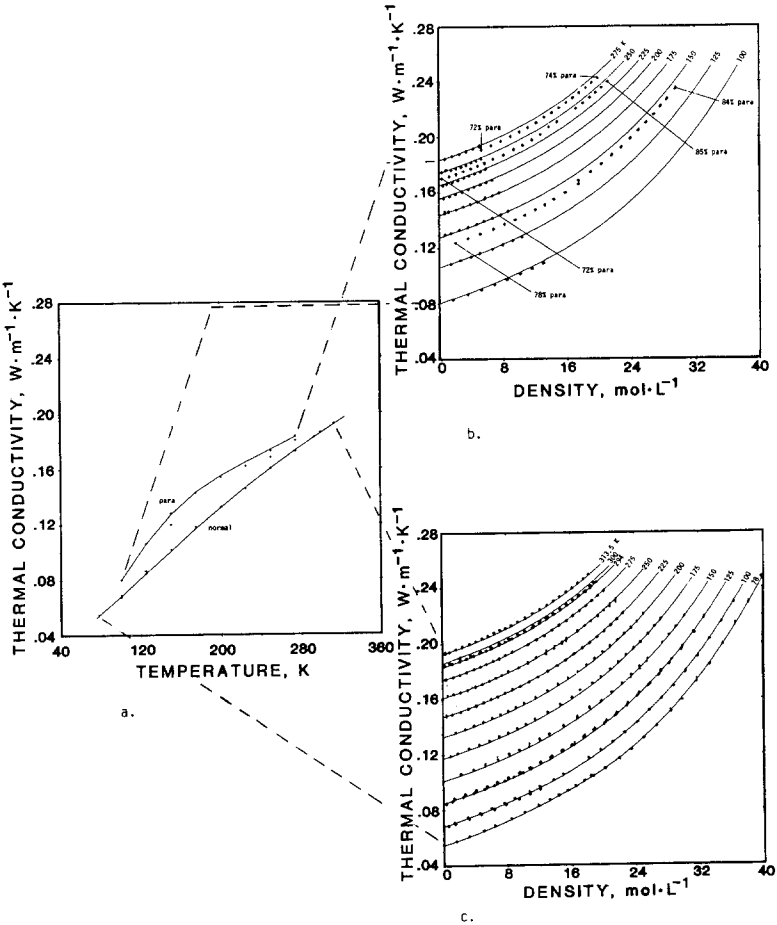

Fig. 1. The thermal conductivity of hydrogen. (a) The dilute gas; (b) para, and para-rich mixtures; (c) normal and near-normal mixtures.

procedure changes the temperature rise in the wire and hence the temperature rise in the gas near the wire. The technique is quite analogous to changing the ΔT for a steady state parallel plate system. Extensive comparisons of the effect of varying the power level for the transient hot wire system were given for N_2 and He in the apparatus paper (Fig. 12 and 15 in ref. [1]) and for argon in Table 2 of ref. [11]. A second argument which implies the absence of convection in the present measurements is to compare them to the best current theoretical predictions. This was done for measurements in the critical region of oxygen [10]. Finally, one can verify the absence of convection experimentally. This was done here in 20 separate runs where the

time to onset of convection is found to be about 5 s. All of the valid runs presented were completed in 0.755 s. We may thus conclude that convection is absent.

4. CORRELATION OF THE THERMAL CONDUCTIVITY SURFACE

It is generally accepted that the thermal conductivity should be correlated in terms of density and temperature [18] rather than temperature and pressure because over a wide range of experimental conditions, the behavior of thermal conductivity is dominated by its density dependence. This preferred technique requires an equation of state [16] to translate measured pressures into equivalent densities. The dependence of thermal conductivity on temperature and density is normally expressed as

$$\lambda(\rho, T) = \lambda_0(T) + \lambda_{\text{excess}}(\rho, T) + \Delta\lambda_{\text{critical}}(\rho, T) \tag{2}$$

The first term on the right of Eq. (2) is the dilute gas term, which is independent of density. The second is the excess thermal conductivity. The first two terms taken together are sometimes called the "background" thermal conductivity. The final term is the critical point enhancement. A slight indication of the critical enhancement appears in the present measurements.

4.1. Term 1: The Dilute Gas

Values for the dilute gas at zero density have been calculated by Hanley et al. [9] using kinetic theory equations for both normal and parahydrogen. The authors present their results in the form of tables, which we will use with a slight modification as shown later on. To obtain a value at zero density from the experiment we must extrapolate the measurements at low densities to zero density, usually with a low order polynominal. This was done with the experimental values after they had been adjusted slightly to fall on even values of temperature. The extrapolations for 26 experimental runs are given in Table IV. They are compared with values obtained from ref [9], taking into account the final ortho-para composition, column 5 in Table IV. The differences, plotted in Fig. 2, are seen to range up to 3% with the experimental values being lower. The line in Fig. 2 shows the best offset considering both normal and para extrapolations. In the new correlation we use the values obtained from the kinetic theory expressions [9] for the λ_0 values of normal hydrogen but lowered by a factor which is temperature dependent and given by

$$F = 1.0 - 0.028484 + 0.000070588\ T \tag{3}$$

Table IV. Extrapolated and Calculated Dilute Gas Thermal Conductivities, λ_0

Run No.	Type	Temperature (K)	Density cutoff (mol · L^{-1})	Para concentration		Dilute gas thermal conductivities, λ_0			
				Initial	Final	Extrapolated (W · m^{-1} · K^{-1})		Calc., ref [9] (W · m^{-1} · K^{-1})	Departures (%)
				Normal and near normal					
45	Long	78.0	11.806	0.2500	0.3564	0.05484	±0.00131	0.05616	−2.42
77	Short	100.0	12.255	0.2500	0.2500	0.06759	±0.00038	0.06950	−2.83
44	Long	100.0	11.974	0.2500	0.3380	0.06903	±0.00046	0.07092	−2.74
75	Short	125.0	8.827	0.2500	0.2500	0.08464	±0.00032	0.08625	−1.91
76	Long	125.0	10.893	0.2500	0.3116	0.08661	±0.00036	0.08801	−1.62
43	Long	125.0	12.115	0.2500	0.3116	0.08619	±0.00106	0.08801	−2.11
42	Long	150.0	13.267	0.2500	0.2815	0.10180	±0.00132	0.10373	−1.90
41	Long	175.0	9.261	0.2500	0.2600	0.11810	±0.00105	0.11920	−0.94
40	Long	200.0	9.103	0.2500	0.2500	0.13253	±0.00078	0.13420	−1.26
50	Long	225.0	7.774	0.2500	0.2500	0.14582	±0.00100	0.14860	−1.91
39	Long	250.0	10.630	0.2500	0.2500	0.16048	±0.00086	0.16220	−1.07
51	Long	275.0	5.513	0.2500	0.2500	0.17281	±0.00155	0.17495	−1.24
48	Long	294.0	6.207	0.2500	0.2500	0.18277	±0.00104	0.18418	−0.77
38	Long	300.0	10.290	0.2500	0.2500	0.18618	±0.00096	0.18700	−0.44
49	Long	313.5	5.718	0.2500	0.2500	0.19268	±0.00219	0.19328	−0.31
				Para and para-rich					
59	Short	100.0	11.642	0.9979	0.9979	0.08009	±0.00052	0.08157	−1.84
58	Short	125.0	10.356	0.9979	0.9979	0.10613	±0.00059	0.10759	−1.38
57	Short	150.0	7.707	0.9979	0.9979	0.12824	±0.00084	0.12932	−0.85
57	Long	150.0	10.746	0.8395	0.7772	0.11999	±0.00039	0.12144	−1.21
56	Short	175.0	7.471	0.9979	0.9979	0.14304	±0.00119	0.14538	−1.63
55	Short	200.0	6.651	0.9979	0.9979	0.15434	±0.00083	0.15733	−1.94
54	Short	225.0	4.476	0.9979	0.9979	0.16223	±0.00288	0.16685	−2.85
53	Short	250.0	5.287	0.9979	0.9979	0.17311	±0.00151	0.17576	−1.53
53	Long	250.0	8.102	0.8478	0.7186	0.16852	±0.00087	0.17070	−1.29
52	Short	275.0	5.072	0.9979	0.9979	0.18372	±0.00460	0.18452	−0.44
52	Long	275.0	12.194	0.7425	0.7157	0.18044	±0.00176	0.18091	−0.26

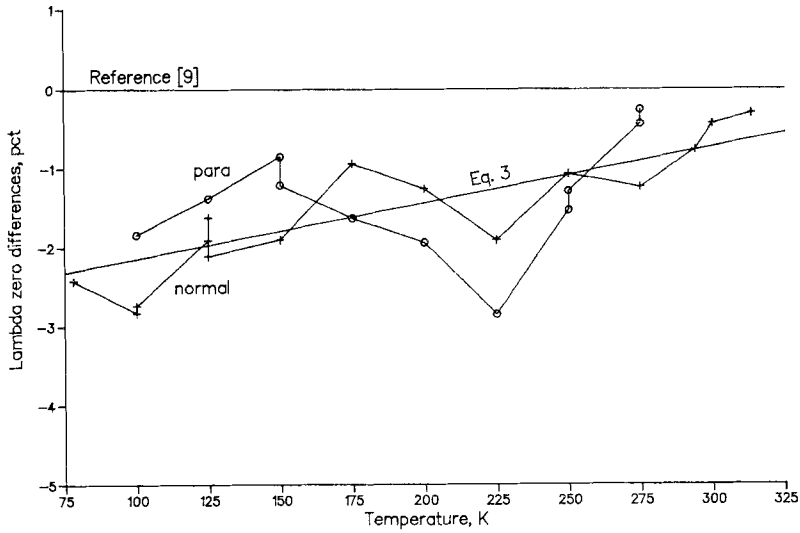

Fig. 2. Differences in dilute gas thermal conductivity, calculated from ref. [9] vs experimental extrapolation.

Use of eq. (3) is justified because the selection of the intermolecular potential and its parameters in [9] is based on the dilute gas viscosities, not the thermal conductivities. This selection introduces a deviation of up to −4% for nearly all available experimental dilute gas thermal conductivities as shown in Fig. 2 and 4 of ref. [9]. To obtain the λ_0 values for parahydrogen we use the revised λ_0's for normal hydrogen and the para-normal difference as given in ref. [9]. Table V shows the values of λ_0 used for normal and parahydrogen in the present correlation.

To account for a variable ortho-para composition, we make the dilute gas term a function of both temperature and ortho-para composition, i.e., $\lambda_0(T)$ becomes $\lambda_0(T, x)$. For a given temperature the relationship is assumed to be linear in composition. It is expressed in Eq. (4) in terms of normal and parahydrogen:

$$\lambda_0(T, x) = \lambda_0(T, 0.25) + [\lambda_0(T, 1.0) - \lambda_0(T, 0.25)](x - 0.25)/0.75 \tag{4a}$$

$$\lambda_0(T, x) = \lambda_0(T, 1.0) - [\lambda_0(T, 1.0) - \lambda_0(T, 0.25)](1.0 - x)/0.75 \tag{4b}$$

where the compositions are given in mole fraction of para.

4.2. Analysis of Ortho-Para Composition

Hydrogen, as measured in this experiment, is a reacting mixture. The ortho-para composition shifts in time toward the equilibrium value [19],

Table V. Dilute Thermal Conductivities, λ_0, Used in the Present Correlation

T (K)	λ_0, normal ($W \cdot m^{-1} \cdot K^{-1}$)	λ_0, para ($W \cdot m^{-1} \cdot K^{-1}$)
70.	0.0493	0.0517
80.	0.0556	0.0605
90.	0.0619	0.0701
100.	0.0681	0.0802
110.	0.0747	0.0908
120.	0.0812	0.1011
130.	0.0879	0.1108
140.	0.0944	0.1195
150.	0.1008	0.1276
160.	0.1073	0.1346
170.	0.1138	0.1408
180.	0.1201	0.1463
190.	0.1263	0.1511
200.	0.1323	0.1555
210.	0.1382	0.1595
220.	0.1439	0.1632
230.	0.1495	0.1668
240.	0.1551	0.1705
250.	0.1604	0.1740
260.	0.1657	0.1776
270.	0.1709	0.1812
280.	0.1759	0.1848
290.	0.1808	0.1884
300.	0.1856	0.1921
310.	0.1904	0.1959
320.	0.1950	0.1998

which depends on the temperature in question. Figure 3 illustrates the detailed experimental situation at 125 K. Runs 75 and 76, series 3, were taken to define the ortho-para conversion in a nominal normal run. Run 76, the long run, is typical of the way in which nearly all of the normal measurements were made. Beginning at the highest density, here 32 mol $\cdot$ L^{-1}, measurements are taken throughout the first day, the system is left overnight, then the measurements are continued for a second day ending at a density near zero. The elasped time was as long as 30 hr. A slight jump in values is noted at a density between 19 and 20 mol $\cdot$ L^{-1} corresponding to the inactive time overnight. Run 75, the short run, is a fresh filling of normal hydrogen at no more than supply tank pressure. A run of this type is completed in 6 hr or less. The two runs are nearly parallel to each other, and the difference between them is interpreted as a change in ortho-para

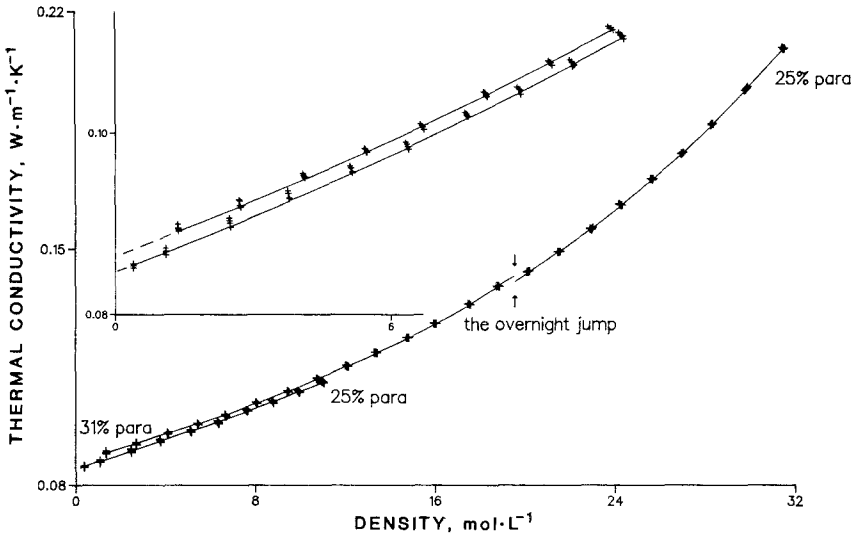

Fig. 3 Ortho-para conversion in "near"-normal runs. Runs 75 and 76 at 125 K.

composition of the long run. We adopt two working hypotheses from the paper of Woolley et al. 19].

Hypothesis 1. The ortho-para composition does not depend on pressure, i.e., the dilute gas thermal conductivities define the ortho-para composition (Eq. 4). This assumption implies that the excess thermal conductivity is independent of ortho-para composition.

Hypothesis 2. The reaction is a second order reaction governed by the equation

$$x/(a(a+x)) = k_2 t \tag{5}$$

where x is the fraction converted, a is the initial concentration, k_2 is the reaction rate constant, and t is the time. If we establish initial and final ortho-para compositions for each run, then Eq. (5) allows us to calculate compositions at intermediate times.

Initial and final compositions for runs or segments of runs are given in Table IV. Most of the initial compositions are defined at filling, 25% para for all normal and near normal runs, and 99.789% para for the short para runs. The initial compositions of the long para-rich runs 57, 53, and 52, were estimated using hypothesis 1 above. A preliminary version of the thermal conductivity surface (Section 4.5) is required. For 10–12 measurements at the highest density, i.e., first in time, the difference between measurement and

a value calculated for normal hydrogen at the experimental density and temperature establish a preliminary value of para composition. The initial composition used for each run is the average of these 10–12 estimates.

Hypothesis 3. Ortho-para conversion occurring during a short run can be neglected. This assumption implies that initial and final compositions for short runs are the same. This assumption is justified experimentally because the reaction rate constants we can calculate are on the order of 0.002 per hour, implying a change of several percent in ortho-para composition during the 6 hr of the short experiments. This change is comparable to the experimental precision in the thermal conductivity measurement.

The final para compositions for runs 44, 76, and 43 were calculated using the λ_0 extrapolations in Table IV as $\lambda_0(T, x)$ and the λ_0 extrapolations of short runs 77 and 75 as $\lambda_0(T, 0.25)$ in Eq. (4a). The results are 0.338, 0.311, and 0.311. These values show that the equilibrium compositions of 0.400, 0.324, and 0.326 were not reached during the experiment. The final para compositions of the long para-rich runs 57, 53, and 52 were estimated in a fashion similar to the one given above for their initial compositions, here using the 8–10 measurements at the lowest densities of each run.

The para compositions given in Table AI for each point were calculated from Eq. (5), the appropriate initial and final compositions for each run, and the experimental times. The times were taken from the experimental log book, setting the start of each run, or segment of a run, equal to zero.

4.3. Term 2: The Excess Thermal Conductivity

The behavior expected of the thermal conductivity surface over a wide range of temperatures and pressures, including the saturation boundary, is discussed in ref. [18]. The range of temperatures covered in the present measurements is 78–315 K. Expressed in terms of the critical temperature, $T_c \simeq 33$ K, the reduced temperature range is $T^* = 2.4$ to about 9.5. Figure 4 contrasts the excess thermal conductivity of normal hydrogen for the extreme temperatures, 78 and 313.5 K. The figure shows that we may not omit or neglect the temperature dependence of the excess thermal conductivity. We make the assumption that the excess thermal conductivity is independent of ortho-para composition within the experimental error.

The functional form used to describe the excess thermal conductivity is similar to the one used for oxygen [10]:

$$\lambda_{\text{excess}}(\rho, T) = \alpha\rho + \delta[e^{\beta\rho^{\gamma}} - 1.0] \tag{6}$$

For oxygen the parameters α, β, γ, and δ are all functions of temperature. For hydrogen since we are in a relatively high reduced temperature range, it

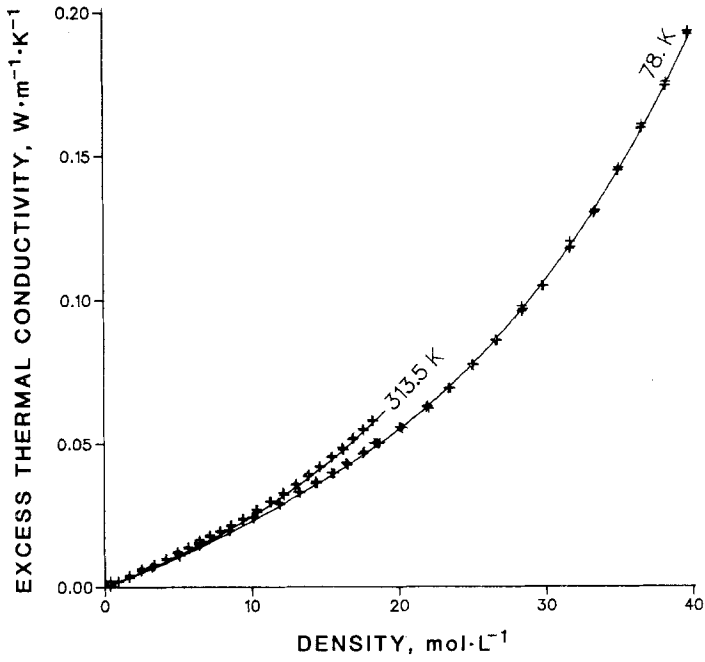

Fig. 4. Temperature dependence of the excess thermal conductivity.

turns out that only the parameter δ has to be a function of temperature. The others α, β, and γ are constant. The coefficients of Eq. (6) are

$$\alpha = 0.15843 \times 10^{-2}, \quad \beta = 2.1, \quad \gamma = 0.36$$

and

$$\delta = (A + BT) = 0.38611 \times 10^{-4} + 0.10664 \times 10^{-7}\, T$$

with λ in $\mathrm{W} \cdot \mathrm{m}^{-1} \cdot K^{-1}$ and ρ in $\mathrm{mol} \cdot \mathrm{L}^{-1}$.

We note that the numerical values for α, β, γ, and δ for hydrogen are quite close to those of oxygen even though the ranges of reduced temperature are considerably different. It would be interesting to investigate the degree to which these two thermal conductivity surfaces obey the principle of corresponding states.

4.4. Term 3: The Critical Enhancement

The existence of a critical enhancement at temperatures up to $2T_c$ has been demonstrated for oxygen [10] and argon [11, 12]. Nevertheless, it is

surprising to find a slight critical enhancement in the present measurements at 78 K, or roughly $2.4T_c$. The indication was discovered during the development of the thermal conductivity surface, which is described in the next section. Using a preliminary version of the new correlation, the departures, experimental minus calculated, for the 78 K isotherm are as shown in Fig. 5a. A term describing the critical enhancement was scaled from oxygen [10]. The reduced variables are $\Delta T = T - T_c$ and $\Delta\rho =$

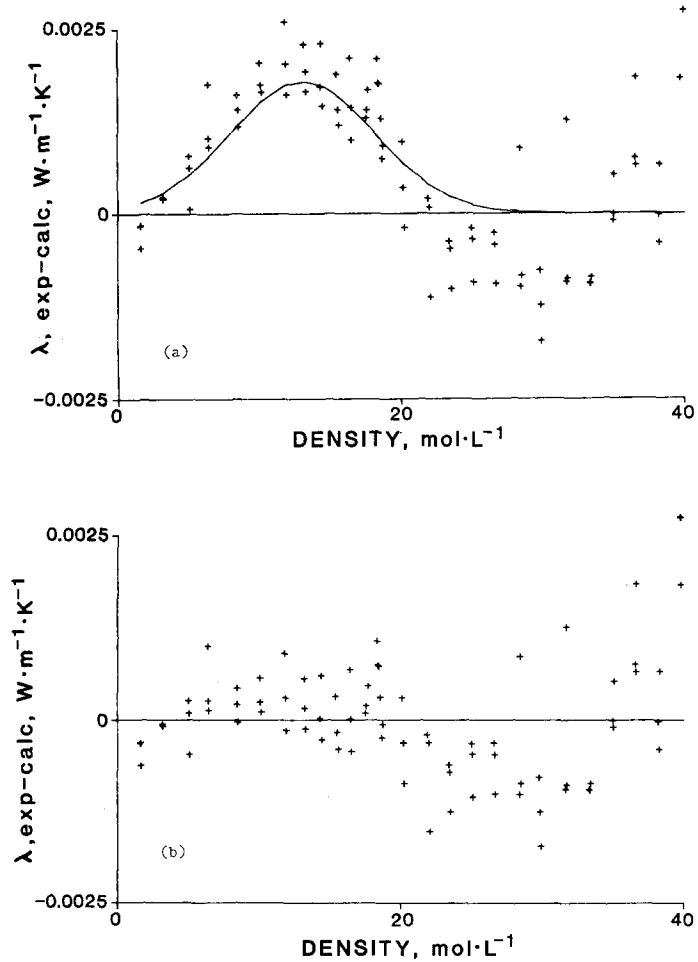

Fig. 5. Indication of a critical enhancement at 78 K. (a) The deviations, experimental-calculated, without the term describing the critical enhancement. The curved line shows the estimated magnitude of $\Delta\lambda_c$. (b) The deviations, experimental-calculated, including a term describing $\Delta\lambda_c$.

$\rho - \rho_{\text{center}}$, where the expression for ρ_{center} is $\rho_{\text{center}} = \rho_c - 0.008229\,\Delta T^{1.5}$. The expression for the critical enhancement becomes

$$\Delta\lambda_{\text{critical}}(\rho, T) = Ae^{-x^2} \tag{7}$$

with the amplitude $A = 0.00635363 - 0.00005863T$, $x = 0.138\Delta\rho$, $T_c = 32.938$ K, and $\rho_c = 15.556$ mol · L^{-1}.

When the critical enhancement, Eq. (7), is included in the description of the thermal conductivity surface, the fit is improved. The revised deviations for the 78 K isotherm are as shown in Fig. 5b.

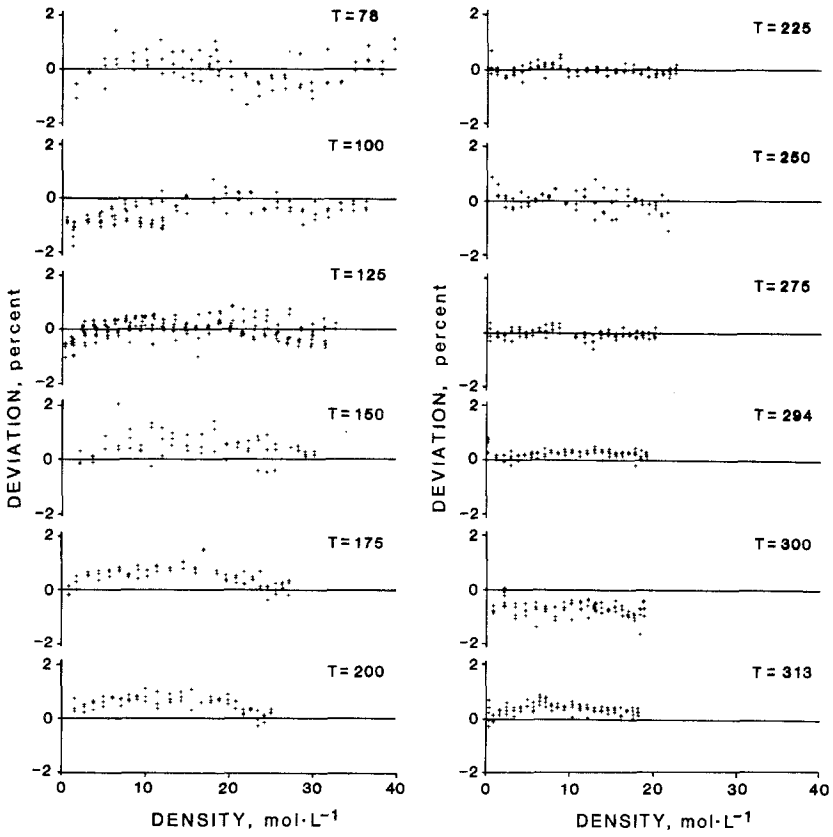

Fig. 6. Deviations of the experimental points from the correlation for normal, and near-normal isotherms.

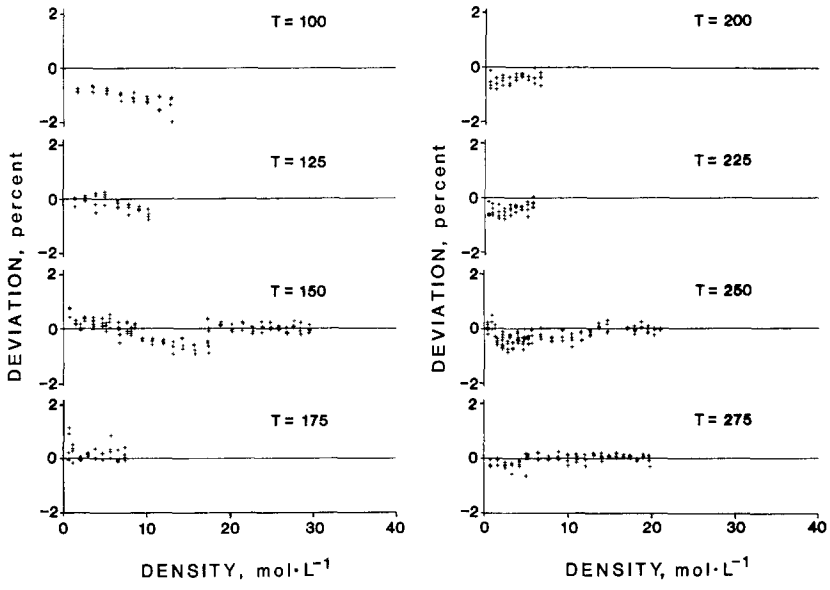

Fig. 7. Deviations of experimental points from the correlation for para and para-rich isotherms.

4.5. The Thermal Conductivity Surface

Equation (2), expressed in detail in Eqs. (3), (4), (6), and (7), describes the thermal conductivity surface of hydrogen for the range of temperatures and pressures measured in this experiment. The entire range of ortho-para compositions is included through Eq. (4), the use of the reduction factor in Eq. (3), and the dilute gas tables from ref. [9] as shown in Table V. The excess thermal conductivity is given by Eq. (6), and the critical enhancement is given as a separate function by Eq. (7). Since the variables normally available to the user are pressure and temperature, an equation of state [16] is required to find the corresponding density.

Deviations between experimental values and the calculated surface are shown for all measurements in Figs. 6 and 7 by isotherms. The surface fit is based on all 1645 points. The average deviation is 0.37%, which is equivalent to 1.5% at the 3 sigma level.

5. DISCUSSION

The precision of the masurements can be established from several considerations. These are the linear regression statistics for a single point, the

variation in the measured thermal conductivity with applied power, and the variation obtained in a curve fit of the thermal conductivity along an isotherm. The precision of the measurements as established by varying the applied power is 0.6% [1, 11]. The reproducibility of the present measurements as seen in Figs. 6 and 7 is about 1.6% for the worst case. For normal hydrogen a systematic deviation of about 1% is noted between the isotherms 300 K, series 1, and 294 K, series 2. The deviations between series 1 and series 3 measurements at 100 and 125 K are seen to be around 1%. These deviations are expected to arise because of changes introduced in the apparatus. The number of points for the wire calibration is not as extensive for series 2 and 3 measurements as it is for series 1. Therefore, wire calibrations are now expresed in terms of a cubic polynomial rather than piecewise parabolic segments. Further, the temperature ranges covered by the wire calibration are different. Series 1 extends to 76 K, series 2 and 3 only to 100 K. On the other end, series 2 and 3 extend to 320 K, series 1 only to 305 K. Resistance corrections for lead wire segments inside the high pressure cell are much more accurately known for the series 2 and 3 measurements. Finally, changes in heater arrangement, thermocouple location, and in the way refrigeration is applied probably also affect the reproducibility.

The accuracy of the apparatus can be established, in principle, from measurements on the rare gases and certain theoretical considerations, i.e., the Eucken factor. For the present results the accuracy was estimated from the variation obtained in the curve fit of the thermal conductivity surface considering different densities, different ortho-para compositions, and different temperatures. This estimate of accuracy is 1.5% (3σ).

Comparisons with the results of others [4, 5, 20] also yield an estimate of accuracy. The comparisons were made through the present correlating surface and are plotted in Fig. 8 for normal hydrogen. The differences are seen to range from +4 to −7%, a full 10% over the surface. The agreement between our earlier results [4], using a different method and an apparatus with an uncertainty of about 2%, and the present ones is within the combined uncertainty of both measurements. We suspect that conversion of normal toward the equilibrium mixture at low temperatures probably occurred in our earlier results considering the long equilibrium times required. The measurements of Golubev and Kal'sina [5] cover the same range of temperature and nearly the same range of densities or pressures as ours but are presented only as a table of smoothed values. The deviations between the two correlations of data are larger than the combined uncertainties and are, furthermore, systematic. The systematic differences arise because the present measurements reveal a distinct dependence on temperature of the λ_{excess}, whereas Golubev and Kal'sina used a single, temperature independent curve to correlate their results. The difference

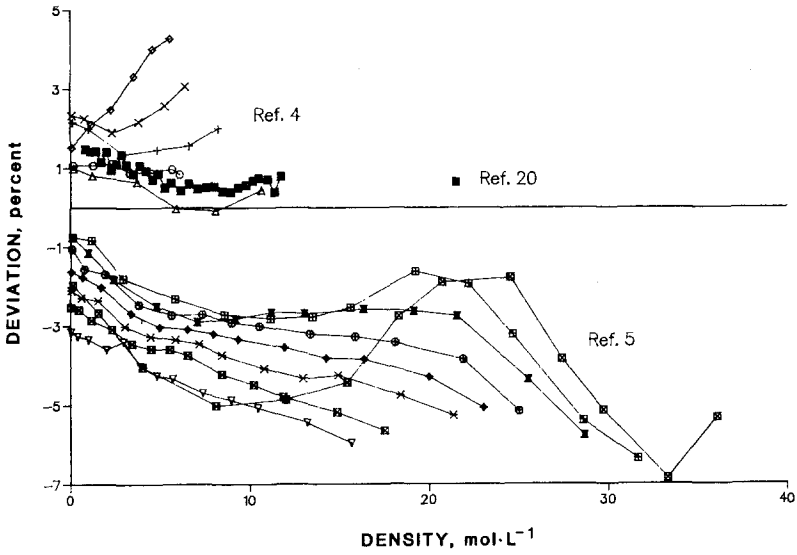

Fig. 8. Comparison of the present correlation with the results of others for normal hydrogen.

between the present results and those of Clifford et al. [20], who also use a transient hot wire method, is around 1.5%, the present results being lower.

The comparison of the present results to those of others for parahydrogen is limited because measurements of the thermal conductivity for this fluid are rare. Our earlier results [4] using a different method and a different apparatus had an uncertainty of about 2%. Using the computer program given in ref. [17], the 17 experimental points given in ref. [4], which fall into the present range of measurements, show an average departure of 1%; thus the two sets of masurements agree well within their combined uncertainty.

Finally, we can compare the present correlation to a previous one by McCarty et al. [6], which considers only data available prior to 1980. At zero density the two surfaces should differ by the factor of Eq. (3). At higher densities the deviations are systematic and run up to 25% percent for both normal and parahydrogen at the lowest temperature of the present measurements, 78 K. The large deviations occur because the previous correlation is extrapolated beyond the range of available data. The situation is illustrated for the 70 MPa isobar and normal hydrogen in Fig. 9. It is clear that a revised correlation for temperatures between 13 and 80 K, or better yet additional measurements at the lower temperatures, are required if we wish to extend the present correlation to lower temperatures.

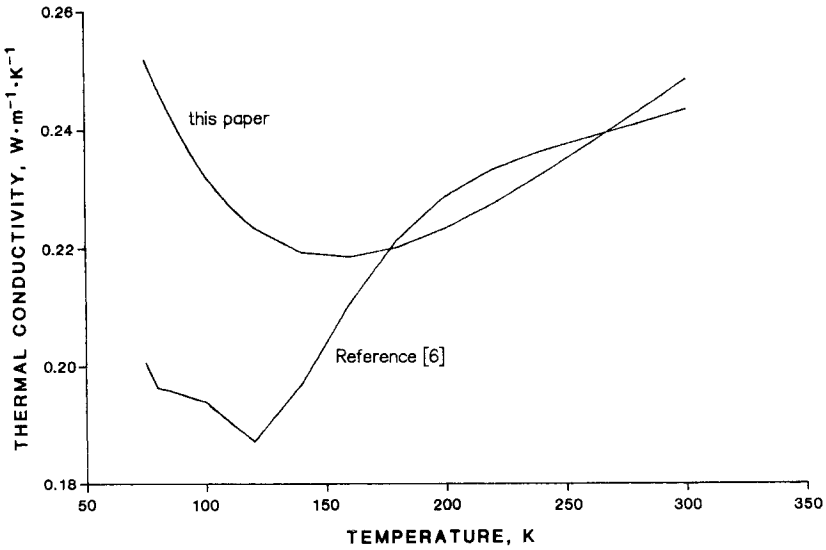

Fig. 9. Comparison of the present correlation to a previous one, ref. [6], for a pressure of 70 MPa. The curve from ref. [6] is a straight line plot between all available table entries.

6. SUMMARY

The thermal conductivity of hydrogen has been measured at temperatures from 78 to 310 K at pressures to 70 PMa. The measurements cover the physical states of the dilute gas, the dense gas, and variations in ortho-para composition. The results were analyzed in conventional terms to develop a mathematical description of the thermal conductivity surface. The accuracy of the present measurements is 1.5% (3σ) as established by the fit of the new correlating surface. The extrapolation of the measured values to zero density and dilute gas values calculated from basic theory and a correlation of the dilute gas values of viscosity differ by up to 3%. The differences between the results of others and the present measurements range between +4 to a mximum of −7%, covering a wide range of temperatures and densities. The present measurements and the new correlation disagree with an extrapolation of an earlier correlation by a maximum of 25%. To extend the present correlation to the triple point temperature will require additional measurements at the lower temperatures.

ACKNOWLEDGMENTS

This work was carried out at the National Bureau of Standards under the sponsorship of the National Aeronautics and Space Administration (C-32369-C).

APPENDIX

Table AI. The Thermal Conductivity of Hydrogen

T (K)	ρ (mol·L^{-1})	Fraction para	$\lambda(T,\rho,x)$ (W·m^{-1}·K^{-1})
normal, near normal, approx. T 78.0			
77.389	39.777	.2505	.2468
77.263	38.252	.2520	.2286
77.542	36.591	.2545	.2139
77.640	35.026	.2573	.1992
77.772	33.378	.2598	.1847
77.896	31.713	.2645	.1730
77.852	29.861	.2647	.1590
78.119	28.459	.2701	.1512
78.044	26.653	.2729	.1402
77.949	25.067	.2754	.1316
78.072	23.486	.2778	.1235
77.958	21.997	.2873	.1169
78.140	20.204	.2859	.1099
78.025	18.681	.2883	.1044
78.266	18.403	.3326	.1047
78.025	17.605	.3343	.1011
78.073	16.485	.3366	.0973
78.161	15.534	.3383	.0941
78.269	14.390	.3401	.0908
78.414	13.250	.3418	.0876
78.313	11.883	.3447	.0837
78.198	10.117	.3466	.0786
78.366	8.491	.3486	.0743
78.425	6.431	.3504	.0694
78.172	5.073	.3522	.0655
78.178	3.206	.3542	.0614
78.546	1.651	.3563	.0582
normal, near normal, approx. T 100.0			
98.748	36.416	.2504	.2286
98.910	34.886	.2526	.2149
99.011	33.406	.2547	.2024
98.883	31.874	.2569	.1898
99.100	30.335	.2602	.1789
99.027	28.843	.2623	.1685
99.175	27.308	.2643	.1596
99.392	25.761	.2667	.1511
99.522	24.255	.2689	.1427
99.401	22.660	.2707	.1352
99.604	21.179	.2725	.1287
99.579	19.662	.3169	.1228
99.660	16.175	.3185	.1172
99.584	14.956	.3223	.1056
99.409	13.749	.3242	.1015
99.566	12.030	.3259	.0967
99.536	10.718	.3283	.0931
99.692	8.914	.3298	.0884
99.439	7.591	.3314	.0850
99.626	6.016	.3330	.0812
99.433	4.567	.3345	.0777
99.748	3.047	.3361	.0747
99.627	1.402	.3378	.0710
103.889	12.092	.2500	.0975
103.661	10.815	.2500	.0939
103.431	9.449	.2500	.0902
103.611	7.806	.2500	.0864
103.390	6.368	.2500	.0828
103.566	4.740	.2500	.0793
103.822	3.206	.2500	.0763
103.675	1.492	.2500	.0727
103.760	.645	.2500	.0713
normal, near normal, approx. T 125.0			
124.469	32.691	.2502	.2184
124.541	31.354	.2516	.2080
124.370	29.989	.2531	.1973
124.440	28.602	.2546	.1878
124.642	27.225	.2567	.1797
124.770	25.857	.2583	.1707
124.794	24.515	.2596	.1640
124.735	23.088	.2609	.1564
124.550	21.715	.2621	.1494
124.732	20.393	.2633	.1440
124.955	18.925	.2958	.1386
125.124	17.630	.2970	.1333
124.829	16.324	.2983	.1274
124.960	14.946	.2996	.1231

[a] T is in K, ρ is in mol · L^{-1}, λ is in W · m^{-1} · K.

Table AI. *(Continued)*

T (K)	ρ (mol·L^{-1})	Fraction para	$\lambda(T,\rho,x)$ (W·m^{-1}·K^{-1})	T (K)	ρ (mol·L^{-1})	Fraction para	$\lambda(T,\rho,x)$ (W·m^{-1}·K^{-1})
124.744	13.580	.3008	.1186	normal, near normal, approx. T 150.0			
124.895	12.155	.3022	.1145	148.110	30.241	.2501	.2183
124.609	10.882	.3036	.1102	148.256	29.179	.2507	.2105
124.635	9.584	.3048	.1073	148.270	28.329	.2512	.2049
124.966	8.136	.3059	.1034	148.657	27.455	.2522	.1995
125.103	6.735	.3071	.1003	148.545	25.581	.2533	.1871
124.953	5.461	.3082	.0971	148.643	24.592	.2538	.1816
125.085	4.033	.3094	.0941	148.785	23.508	.2544	.1759
124.846	2.758	.3104	.0913	148.913	22.348	.2549	.1700
125.217	1.388	.3115	.0883	148.973	21.082	.2555	.1640
126.391	31.482	.2502	.2090	149.167	19.745	.2561	.1577
126.297	29.849	.2517	.1970	149.032	18.291	.2746	.1529
126.416	28.334	.2532	.1866	149.121	16.757	.2752	.1463
126.263	26.994	.2545	.1780	149.269	15.038	.2758	.1401
126.364	25.656	.2561	.1705	149.084	13.230	.2763	.1342
126.569	24.253	.2576	.1629	149.202	12.047	.2769	.1305
126.323	22.955	.2590	.1558	149.288	10.770	.2774	.1269
126.417	21.522	.2604	.1491	149.474	9.509	.2780	.1231
126.293	20.159	.2618	.1432	149.201	8.229	.2793	.1200
126.485	18.801	.2936	.1388	149.340	6.810	.2799	.1169
126.565	17.519	.2949	.1335	149.128	5.249	.2804	.1127
126.352	16.009	.2961	.1277	149.218	3.754	.2809	.1089
126.475	14.789	.2974	.1236	149.110	2.212	.2814	.1057
126.554	13.376	.2987	.1191				
126.266	12.113	.3002	.1151				
126.491	10.774	.3014	.1114	normal, near normal, approx. T 175.0			
126.236	9.461	.3028	.1077				
126.298	8.062	.3046	.1042	174.162	27.267	.2501	.2169
126.029	6.684	.3059	.1007	174.427	26.495	.2502	.2120
126.174	5.459	.3071	.0980	174.447	25.701	.2506	.2066
126.318	4.115	.3089	.0952	174.552	24.727	.2509	.2006
126.136	2.718	.3100	.0923	174.687	23.839	.2510	.1962
126.352	1.376	.3115	.0895	174.742	22.946	.2512	.1915
125.933	10.999	.2500	.1106	174.410	21.944	.2514	.1859
126.002	9.937	.2500	.1076	174.519	20.940	.2516	.1810
126.109	8.793	.2500	.1047	174.680	19.755	.2518	.1755
126.276	7.658	.2500	.1020	174.810	18.649	.2519	.1711
125.888	6.357	.2500	.0986	174.553	17.129	.2576	.1661
126.081	5.145	.2500	.0959	174.611	16.080	.2578	.1608
126.265	3.789	.2500	.0931	174.693	14.636	.2579	.1559
126.023	2.498	.2500	.0902	174.351	13.070	.2581	.1501
125.819	1.112	.2500	.0870	174.625	11.472	.2583	.1453
125.970	.404	.2500	.0855	174.731	10.348	.2585	.1418

[a] T is in K, ρ is in mol · L^{-1}, λ is in W · m^{-1} · K^{-1}.

Table AI. *(Continued)*

T (K)	ρ (mol·L^{-1})	Fraction para	$\lambda(T,\rho,x)$ (W·m^{-1}·K^{-1})
174.788	9.239	.2586	.1388
174.997	8.108	.2589	.1357
174.609	7.005	.2591	.1330
174.759	5.807	.2593	.1301
174.971	4.519	.2595	.1272
174.557	3.246	.2596	.1242
174.911	1.848	.2598	.1212
174.592	.954	.2600	.1189
normal, near normal, approx. T 200.0			
200.316	25.113	.2500	.2215
200.212	24.314	.2500	.2160
200.360	23.538	.2500	.2115
200.443	22.696	.2500	.2075
200.510	21.829	.2500	.2026
200.632	20.904	.2500	.1986
200.690	19.969	.2500	.1943
200.573	18.937	.2500	.1894
200.205	17.939	.2500	.1847
200.291	16.807	.2500	.1798
200.343	15.607	.2500	.1753
200.381	14.362	.2500	.1709
200.182	13.049	.2500	.1661
200.295	11.556	.2500	.1612
200.448	10.098	.2500	.1573
200.130	9.105	.2500	.1542
200.113	8.144	.2500	.1515
200.228	7.194	.2500	.1490
199.885	6.161	.2500	.1465
200.006	5.067	.2500	.1437
200.145	3.890	.2500	.1410
200.333	2.806	.2500	.1387
200.028	1.633	.2500	.1362
normal, near normal, approx. T 225.0			
225.409	22.555	.2500	.2222
225.745	21.812	.2500	.2180
225.761	21.017	.2500	.2138
225.783	20.201	.2500	.2096
225.850	19.294	.2500	.2052
225.950	18.378	.2500	.2011
226.027	17.448	.2500	.1973
226.151	16.420	.2500	.1931
226.214	15.363	.2500	.1888
225.851	14.317	.2500	.1846
225.946	13.123	.2500	.1806
226.009	11.881	.2500	.1765
226.081	10.755	.2500	.1729
225.749	9.682	.2500	.1696
225.425	8.726	.2500	.1673
225.405	7.802	.2500	.1646
225.388	6.872	.2500	.1621
224.974	6.055	.2500	.1600
225.018	5.136	.2500	.1577
225.130	4.178	.2500	.1553
225.186	3.178	.2500	.1532
225.679	2.218	.2500	.1512
225.222	1.175	.2500	.1492
224.831	.466	.2500	.1479
normal, near normal, approx. T 250.0			
249.683	21.647	.2500	.2308
249.870	20.910	.2500	.2275
249.977	20.185	.2500	.2240
249.950	19.421	.2500	.2200
250.049	18.552	.2500	.2163
250.126	17.755	.2500	.2129
249.735	16.866	.2500	.2090
249.884	15.478	.2500	.2029
249.966	14.922	.2500	.2004
249.997	13.963	.2500	.1971
250.119	12.926	.2500	.1937
249.682	11.679	.2500	.1898
249.805	10.651	.2500	.1861
249.956	9.461	.2500	.1825
250.170	8.181	.2500	.1800
249.724	7.416	.2500	.1772
249.723	6.627	.2500	.1752
249.809	5.795	.2500	.1729
249.875	4.957	.2500	.1709
249.989	4.098	.2500	.1691
249.570	3.109	.2500	.1664
249.682	2.236	.2500	.1649

[a] T is in K, ρ is in mol · L^{-1}, λ is in W · m^{-1} · K^{-1}.

Table AI. *(Continued)*

T (K)	ρ (mol·L^{-1})	Fraction para	$\lambda(T,\rho,x)$ (W·m^{-1}·K^{-1})
249.619	1.339	.2500	.1635
249.363	.611	.2500	.1628
normal, near normal, approx. T 275.0			
274.441	20.141	.2500	.2379
274.406	19.413	.2500	.2341
274.384	18.692	.2500	.2305
274.387	17.938	.2500	.2269
274.409	17.129	.2500	.2234
274.360	16.323	.2500	.2200
274.415	15.471	.2500	.2161
274.453	14.580	.2500	.2129
274.519	13.663	.2500	.2094
274.124	12.725	.2500	.2052
274.179	11.752	.2500	.2023
274.232	10.670	.2500	.1989
273.473	8.730	.2500	.1933
273.310	7.865	.2500	.1909
273.285	7.069	.2500	.1885
273.472	6.329	.2500	.1867
274.122	5.494	.2500	.1848
273.929	4.712	.2500	.1828
273.969	3.953	.2500	.1813
274.082	3.004	.2500	.1790
274.197	2.164	.2500	.1772
274.378	1.333	.2500	.1757
273.944	.440	.2500	.1738
normal, near normal, approx. T 294.0			
296.050	19.231	.2500	.2455
295.750	18.595	.2500	.2420
295.746	17.895	.2500	.2388
295.915	17.126	.2500	.2355
295.964	16.343	.2500	.2320
295.978	15.573	.2500	.2286
296.043	14.784	.2500	.2256
295.974	13.944	.2500	.2222
296.125	13.037	.2500	.2192
296.196	12.139	.2500	.2158
296.250	11.265	.2500	.2128
296.317	10.328	.2500	.2100
296.381	9.490	.2500	.2073
296.205	8.655	.2500	.2047
296.979	7.817	.2500	.2028
296.763	7.069	.2500	.2006
296.821	6.202	.2500	.1983
296.679	5.493	.2500	.1965
297.012	4.636	.2500	.1945
296.577	3.909	.2500	.1925
296.666	3.033	.2500	.1905
296.836	2.194	.2500	.1888
296.959	1.269	.2500	.1870
297.046	.268	.2500	.1860
normal, near normal, approx. T 300.0			
299.220	18.915	.2500	.2435
298.690	18.458	.2500	.2402
298.692	17.751	.2500	.2368
298.738	17.022	.2500	.2337
298.843	16.312	.2500	.2310
298.787	15.478	.2500	.2277
298.972	14.676	.2500	.2243
299.028	13.835	.2500	.2212
299.042	12.963	.2500	.2181
298.481	13.119	.2500	.2185
298.731	12.245	.2500	.2155
298.751	11.353	.2500	.2126
298.805	10.248	.2500	.2089
298.382	9.370	.2500	.2061
298.388	8.287	.2500	.2025
298.534	7.132	.2500	.1997
298.667	5.992	.2500	.1967
298.874	4.763	.2500	.1939
298.987	3.527	.2500	.1911
298.972	2.226	.2500	.1887
299.126	2.213	.2500	.1897
298.615	.897	.2500	.1855
normal, near normal, approx. T 313.5			
314.103	18.257	.2500	.2502
313.490	17.631	.2500	.2469
313.469	16.926	.2500	.2437

[a] T is in K, ρ is in mol · L^{-1}, λ is in W · m^{-1} · K^{-1}.

Table AI. *(Continued)*

T (K)	ρ (mol·L^{-1})	Fraction para	$\lambda(T,\rho,x)$ (W·m^{-1}·K^{-1})
313.564	16.204	.2500	.2402
313.598	15.444	.2500	.2374
313.639	14.644	.2500	.2340
313.665	13.861	.2500	.2309
313.761	13.026	.2500	.2279
313.805	12.179	.2500	.2248
313.849	11.292	.2500	.2220
313.902	10.370	.2500	.2190
313.848	9.420	.2500	.2160
313.901	8.601	.2500	.2137
314.007	7.875	.2500	.2116
313.175	7.171	.2500	.2097
313.124	6.454	.2500	.2079
313.175	5.703	.2500	.2054
313.117	4.957	.2500	.2038
313.227	4.180	.2500	.2017
313.335	3.388	.2500	.1997
313.418	2.506	.2500	.1980
313.526	1.681	.2500	.1961
312.960	.919	.2500	.1938
312.607	.386	.2500	.1929
para, para-rich, approx. T 100.0			
99.373	12.991	.9979	.1087
99.391	11.576	.9979	.1047
99.495	10.107	.9979	.1010
99.368	8.464	.9979	.0968
99.470	6.921	.9979	.0932
99.278	5.275	.9979	.0895
99.453	3.580	.9979	.0861
99.390	1.748	.9979	.0823
para, para-rich, approx. T 125.0			
124.232	10.318	.9979	.1274
124.351	9.182	.9979	.1248
124.475	7.949	.9979	.1219
124.586	6.634	.9979	.1190
124.330	5.104	.9979	.1156
124.501	3.990	.9979	.1133
124.672	2.710	.9979	.1109
124.528	1.469	.9979	.1083
para, para-rich, approx. T 150.0			
148.898	8.634	.9979	.1456
148.950	7.681	.9979	.1432
149.044	6.665	.9979	.1408
149.123	5.615	.9979	.1388
148.834	4.722	.9979	.1364
148.955	3.624	.9979	.1343
149.059	2.567	.9979	.1323
148.883	1.524	.9979	.1299
148.897	.794	.9979	.1291
149.144	29.583	.8394	.2346
149.232	28.506	.8378	.2269
149.280	27.689	.8363	.2217
149.026	26.876	.8350	.2156
149.140	25.905	.8337	.2098
149.244	24.938	.8323	.2042
148.940	23.918	.8310	.1981
149.048	22.772	.8295	.1918
149.145	21.582	.8280	.1862
148.937	20.303	.8267	.1797
149.043	18.935	.8254	.1740
149.163	17.424	.8241	.1679
149.186	17.419	.7907	.1654
148.860	15.774	.7896	.1588
148.941	14.337	.7884	.1541
148.875	13.206	.7871	.1501
148.934	12.029	.7859	.1467
149.086	10.713	.7844	.1430
149.185	9.499	.7831	.1398
148.904	8.166	.7820	.1364
149.018	6.800	.7808	.1329
149.170	5.153	.7795	.1297
148.935	3.645	.7783	.1262
149.198	2.082	.7773	.1232
para, para-rich, approx. T 175.0			
173.581	7.493	.9979	.1591
173.635	6.653	.9979	.1569
173.641	5.740	.9979	.1553
173.753	4.806	.9979	.1528
173.857	3.953	.9979	.1510

[a] T is in K, ρ is in mol · L^{-1}, λ is in W · m^{-1} · K^{-1}.

Table AI. *(Continued)*

T (K)	ρ (mol·L^{-1})	Fraction para	$\lambda(T,\rho,x)$ (W·m^{-1}·K^{-1})
173.954	3.050	.9979	.1492
174.159	2.159	.9979	.1473
173.545	1.219	.9979	.1455
173.316	.729	.9979	.1448
para, para-rich, approx. T 200.0			
199.473	6.631	.9979	.1688
199.533	5.890	.9979	.1671
199.581	5.155	.9979	.1654
199.648	4.398	.9979	.1639
199.314	3.688	.9979	.1620
199.409	2.909	.9979	.1602
199.473	2.077	.9979	.1586
199.117	1.334	.9979	.1569
199.081	.601	.9979	.1554
para, para-rich, approx. T 225.0			
224.014	5.824	.9979	.1767
224.031	5.176	.9979	.1749
224.107	4.464	.9979	.1733
224.144	3.752	.9979	.1718
224.244	3.115	.9979	.1704
224.332	2.402	.9979	.1686
223.967	1.716	.9979	.1672
223.866	.977	.9979	.1658
223.904	.526	.9979	.1649
para, para-rich, approx. T 250.0			
254.747	21.097	.8473	.2420
255.019	20.345	.8443	.2380
254.808	19.594	.8415	.2341
254.820	18.826	.8367	.2307
254.952	18.019	.8337	.2265
254.991	17.139	.8310	.2227
254.698	14.755	.8278	.2129
254.731	13.740	.8250	.2091
254.778	12.688	.7507	.2036
254.664	11.622	.7484	.1997
254.288	10.475	.7460	.1957
254.326	9.349	.7438	.1927
254.463	8.074	.7412	.1888
254.491	6.762	.7383	.1857
254.570	5.693	.7337	.1830
254.412	4.838	.7315	.1808
254.549	4.003	.7291	.1789
254.596	3.084	.7269	.1769
254.691	2.192	.7245	.1749
254.730	1.289	.7219	.1734
254.329	.395	.7185	.1718
253.514	5.270	.9979	.1858
253.351	4.644	.9979	.1841
253.356	4.040	.9979	.1829
253.291	3.395	.9979	.1811
253.446	2.791	.9979	.1798
253.544	2.156	.9979	.1786
253.614	1.535	.9979	.1776
253.491	.927	.9979	.1776
253.195	.407	.9979	.1760
para, para-rich, approx. T 275.0			
273.045	19.836	.7423	.2420
273.135	19.102	.7405	.2387
273.675	18.368	.7386	.2350
273.467	17.539	.7368	.2313
273.495	16.747	.7351	.2278
273.555	15.908	.7333	.2244
273.602	15.022	.7315	.2206
273.203	14.121	.7297	.2169
273.241	13.181	.7280	.2137
273.378	12.165	.7262	.2097
273.468	11.126	.7244	.2064
273.502	10.084	.7227	.2031
273.617	8.948	.7210	.2000
273.210	7.767	.7193	.1964
273.329	6.529	.7175	.1933
273.464	5.306	.7159	.1903
272.730	5.059	.9979	.1929
272.794	4.282	.9979	.1909
272.846	3.390	.9979	.1887
272.895	2.558	.9979	.1870
273.211	1.670	.9979	.1856
272.652	.800	.9979	.1834

[a] T is in K, ρ is in mol · L^{-1}, λ is in W · m^{-1} · K^{-1}.

REFERENCES

1. H. M. Roder, *J. Res. Natl. Bur. Stand. (U.S.)* **86**:457 (1981).
2. A. Farkas, *Orthohydrogen Parahydrogen and Heavy Hydrogen* (Cambridge University Press, London, 1935).
3. R. D. McCarty, *Hydrogen-Technological Survey-Thermophysical Properties.* National Aeronautics and Space Administration, NASA SP-3089 (1975), appendices 6.1 and 6.2.
4. H. M. Roder and D. E. Diller, *J. Chem. Phys.* **52**:5928 (1970).
5. I. F. Golubev and M. V. Kal'sina, *Gazov. Prom.* **9**:41 (1964).
6. R. D. McCarty, J. Hord, and H. M. Roder, Natl. Bur. Stand. (U.S.), Monogr. 168 (1981).
7. H. M. Roder, in *Proc. Int. Therm. Cond. Conf. 17th*, J. G. Hust, ed. (Plenum, New York, 1983), p. 257.
8. H. M. Roder, *J. Chem. Eng. Data* **29**:382 (1984).
9. H. J. M. Hanley, R. D. McCarty, and H. Intemann, *J. Res. Natl. Bur. Stand. (U.S.)* **74A**:331 (1970).
10. H. M. Roder, *J. Res. Natl. Bur. Stand (U.S.)* **87**:279 (1982).
11. C. A. N. de Castro and H. M. Roder, *J. Res. Natl. Bur. Stand. (U.S.)* **86**:293 (1981).
12. C. A. N. de Castro and H. M. Roder, *Proc. 8th Symp. Thermophys. Prop.*, J. V. Sengers, ed. (ASME, New York, 1982), p. 241.
13. H. M. Roder and C. A. N. de Castro, *J. Chem. Eng. Data* **27**:12 (1982).
14. H. M. Roder, submitted to *Int. J. Thermophys.*
15. J. R. Purcell and R. N. Keeler, *Rev. Sci. Instrum.* **31**:304 (1960).
16. R. D. McCarty, Natl. Bur. Stand. (U.S.), Tech. Note 1025 (1980).
17. H. M. Roder, Experimental thermal conductivity measurements on hydrogen, methane, and ethane, Nat. Bur. Stand. (U.S.) Interagency Report NBSIR 84-3006 (1984).
18. D. E. Diller, H. J. M. Hanley, and H. M. Roder, *Cryogenics* **10**:286 (1970).
19. H. W. Woolley, R. B. Scott, and F. G. Brickwedde, *J. Res. Natl. Bur. Stand. (U.S.)* **41**:379 (1948).
20. A. A. Clifford, J. Kestin, and W. A. Wakeham, *Ber. Bunsenges. Phys. Chem.* **84**:9 (1980).